Karlsruhe Institute of Technology

KSOP
Karlsruhe School of Optics & Photonics

Direct Laser Writing and Scanning Electron Microscopy Laboratory

Report

14 December 2016

Daniel Lechner 1938869
Velat Kiliç 2080642
Arash Aghigh 2085885

Contents

1 Introduction

Two-Photon absorption (TPA) Laser Microfabrication is among one of the most advanced microfabrication techniques which can be used to design and realize microstructures by using a femtosecond laser. One of the interesting aspects of this type of microfabrication technique is that because of nonlinear processes the resolution can exceed the diffraction limit by controlling the parameters of the laser such as the energy and number of applied laser pulses. It also provides the capability to confine photochemical and physical reactions which is of great importance as well. 3D structures are are also realizable by direct laser writing which is in high demand and will gradually grow to be used in the industry as the need for well defined nanostructures is increasing day by day and thus this can be a viable solution to the problem.
Another important aspect is to analyze created structures in terms of shape, size, defects and other criteria which are important and can vary in different projects. One of the most well established methods for measuring nano and sub-micron structures is scanning electron microscopy (SEM) which is extensively used in many areas in the industry. Its advantages over optical microscopes is that it provides far better resolution and magnification and provides high depth of focus.
In this lab firstly, a microstructure will be formed using the TPA method mentioned above and afterwards the functionality of a SEM device will be explored extensively and will also be used to measure the size of the created microstructure as well as the diameter of the voxel arrays on the substrate.

2 Theory

In this section of the report, the theory involved around the experiment and the SEM device will be briefly discussed.

2.1 Two Photon Absorption Direct laser Writing

For creating structures in the sub-micron and nano-scale, direct laser writing method based on two photon absorption can be used. Before we can further dive into the direct laser writing we should first have a look at the two photon absorption process. As from its name suggests, two photon absorption is the process of absorbing two photons simultaneously to excite a molecule from the ground state to an excited state. This process is very much energy dependent and thus the intensity of the light plays an important role in this process. Another important aspect of such process is the Two Photon Absorption threshold, which is not only related to the laser functionality and performance but also the material property which is being used for the photo polymerization process. The intensity of the laser should surpass the TPP threshold value for the polymerization to occur. As an example and for further illustration, The graph below can be used:

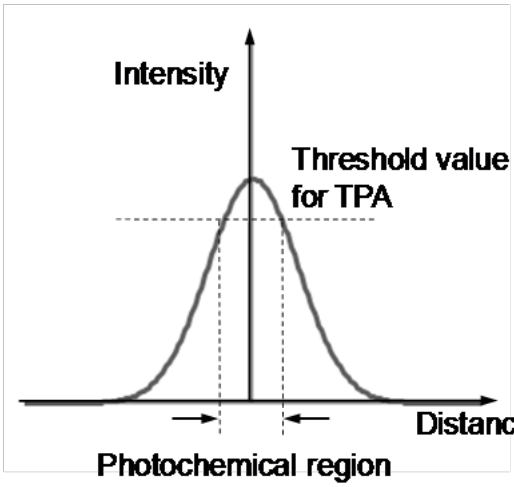

Figure 2.1: Polymerization only occurs where the intensity of the laser surpasses the TPP threshold [5]

Now that we have a basic understanding of TPA, direct laser writing can be described. In this method, a femto-second laser is tightly focused onto a transparent photoresist and this action will create radicals which causes polymerization on the places where the laser is applied

and hence the name photopolymerization. However, for this process to occur, some special molecules called photoinitiators are used to facilitate the photopolymerization which causes the solidification of photoresist when the laser is applied. One could ask why it is that a two photon process is used instead of a single photon one. The reason is that when one highly energetic photon is absorbed, it will penetrate the photoresist's surface by only a few micrometers whereas when we are using two photon absorption with smaller energies, the photons can penetrate the photoresist deeper and create 3D structures[4][7][6].
There are two types of scanning methods that can be used for the process: raster and vector scanning modes. Vector scanning mode is more suitable when less exposure time is required and simple structures are needed. Raster scanning is used for making high accuracy and more complex structures [7] and these two kinds of scanning methods can be seen in figure2.2:

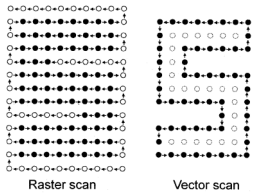

Figure 2.2: Raster and Vector mode[7]

As an approximation, the voxel length and diameter and its relation to the laser power can be summarized [6]:

$$l(N_0,t) = 2z_R[(\frac{\sigma_2 N_0^2 n\tau_L}{C})^{\frac{1}{2}} - 1]^{\frac{1}{2}}$$

Where z_R is the Rayleigh length, σ_2 is the effective two-photon cross section for the generation of radicals, n is the number of laser pulses and τ_L is the laser pulse duration and the C can be is given by:

$$C = ln[\frac{\rho_0}{(\rho_0 - \rho_{th})}]$$

In which ρ_0 is primary initiator particle density and the ρ_{th} is the polymerization threshold. In addition, the formula for N_0 can be given by:

$$N_0 = \frac{2}{\pi r_0^2 \tau_L}\frac{PT}{v\hbar\omega_L}$$

where, P is the average laser power and T is the fraction transmission of light through the objective.
Moreover, the equation for the diameter of a voxel is also given by:

$$d(N_0,t) = r_0[ln(\frac{\sigma_2 N_0^2 n\tau_L}{C}]^{\frac{1}{2}}$$

from the equation given it can be clearly seen that the diameter of the voxel is related to many parameters of the experiment in which is being conducted, such as the effective two-photon

cross section for the generation of radicals, number of laser pulses, laser-pulse duration and photon flux, which in terms are also closely related to the length of the voxel which was briefly discussed previously.

2.2 Resolution Limit

For any optical system, there exists an unbeatable resolution limit due to diffraction from the aperture. Sometimes use tricks can be used to work around the diffraction limit such as stimulated emission from fluorophores. In our case, trick involves controlling the light intensity and making use of the polymerization threshold to obtain voxels comparable to or even smaller than the diffraction limit.
The diffraction resolution limit of our optical system is determined by the Rayleigh criterion. 2 point sources imaged by a circularly symmetric optical system will have their intensities described by 2 Airy functions in the image plane. Rayleigh criterion states that these 2 point sources can be resolved as long as the maximum intensity of one of them doesn't coincide with the first minimum of the other as seen in Figure 2.3

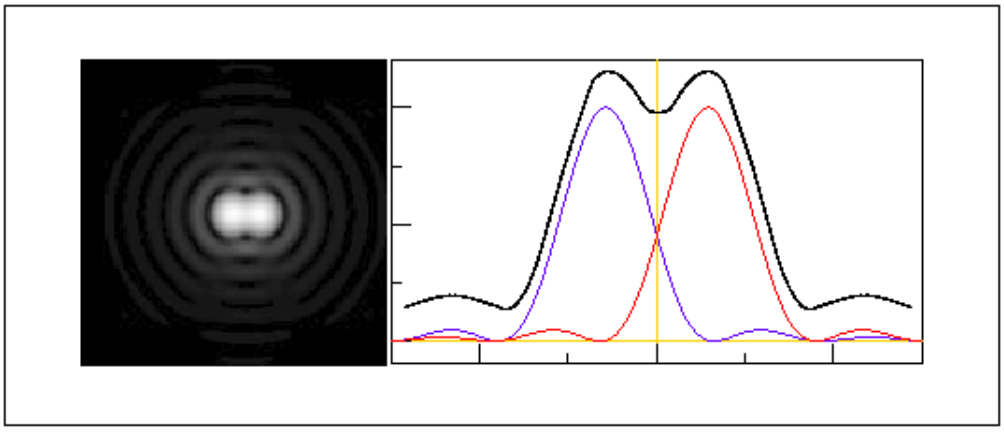

Figure 2.3: Airy functions on the image plane demonstrating the Rayleigh criterion [3]

The minimum resolvable angle on the image side is:

$$\theta_{airy} \approx 1.22\frac{\lambda}{D}$$

where λ is the wavelength and D is the diameter of the diffracting aperture. Then, the minimum resolvable distance in the object plane can be calculated:

$$d = \frac{\lambda}{2nsin(\alpha)} = \frac{\lambda}{2NA}$$

where NA is the numerical aperture.

2.3 Scanning Electron Microscopy (SEM)

Compared to optical methods, SEM can resolve smaller features due to small wavelength of the electrons and that's why we use it to measure voxel dimensions. An SEM has an electron source, and electromagnetic components for electron beam guidance and a detection scheme as seen in figure 2.4:

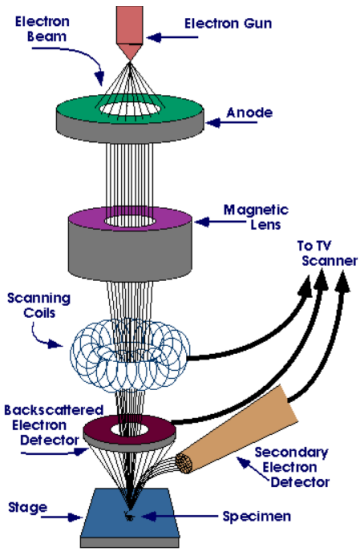

Figure 2.4: Scanning Electron Microscopy[1]

If we break down the device from top to bottom we should start first with the electron gun of the device. An electron gun is a cathode which shoots a stream of electrons generated by thermionic emission. The second part of the SEM consists of condenser apertures which is used to focus the stream of electrons at the substrate. These apertures are magnetic induction coils, in which by applying a current to this apertures, it will focus or de-focus the stream of electrons. Afterwards, a deflection coil is used so that the electron coil can scan the substrate. Then, the secondary electrons from the substrate are captured using a special detector named Everhart-Thornley Detector. The scattered electrons can be used to generate an image of the surface topography of the sample[4][1].
Basically when the electron hits the surface of a substrate, many interaction can occur which can be summarized in the illustration below:

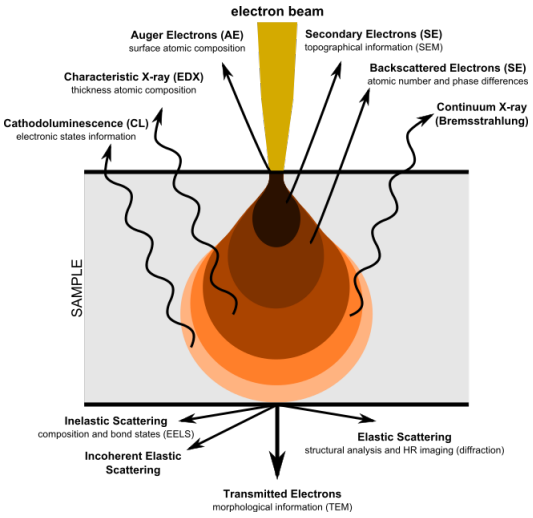

Figure 2.5: Electron Interaction with sample[2]

So an ordinary SEM will produce phenomena when the electron ray interacts with the material: the specimen itself emits secondary electrons, some of the primary electrons are reflected from the specimen which are also called backscattered electrons, electrons can be absorbed by the specimen in which will cause the specimen to emit either X-ray or photons or be lose its energy through phonon but the two most important phenomena that we are most interested are secondary electrons and backscattered electrons. Secondary electron is an inelastic process in which an incident electron which passes through the specimen's atom will ionize an electron and this ionized electron in which leaves the specimen is called the secondary electron. These secondary electrons are tightly related to the topography of the surface of the specimen and some parts of the specimen will produce more secondary electrons than other parts of the sample and for further illustration the figure below can be used to identify this process:

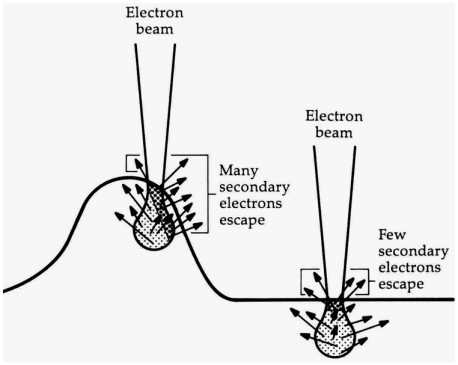

Figure 2.6: Secondary electrons from different parts of the sample[1]

Another phenomenon that occurs with an ordinary SEM is the Backscattered electrons. BSE is produced by an elastic process in which the incident electrons are slingshot back when colliding with the nucleus. Although they are favorable for material composition detection, but for simple SEM they are the main source of noise which will cause the image to be not as crisp

as wanted[1].
The resolution of a SEM is limited by the elctron probe size which is dependent on the objective lens and the electron gun and the equation for the resolution of a SEM is given by the diffraction limit equation:

$$d_d = \frac{1.22\lambda}{D}$$

in which λ is the wavelength of the incident beam and D is the diameter of the lens being used. In addition, another aspect which cannot be overlooked is the fact that the PC screen display also plays an important role and the resolution cannot go further than one pixel on the PC screen display. Moreover, Depth of Field is defined as the distance parallel to the optical axis of the microscope that a feature on the specimen can be displaced without loss of resolution which can be given by the equation below:

$$DOF = \frac{0.1mm}{M\alpha}$$

In which 0.1mm is the smallest detail a human eye can spot, M is the total magnification of the SEM and α is the angle of deflection from the lens to the specimen[1].

3 Methods

In this chapter, the performed experiment will be completely explained so that the reader can have a step by step guide on each and every part of the experiment starting from the fabrication point of view, down to the SEM analysis of the created structure.
As for the sample preparation, a resist was applied to a glass substrate. Thus, the first step of the sample preparation was to clean the glass substrate thoroughly and afterwards by the usage of a spin coating device at different speeds. The glass substrate was coated with the resist and then exposed to the femto-second laser. With the vector scan method, LTI logo was printed on the sample with the computer generated voxel pattern. For better results, before developing the sample, a baking was performed right after the TPA process and then development of the sample took place. Sample was baked once more with a higher temperature for a hard bake [4]. In the end, the sample was coated with gold in preparation for the analysis in the scanning electron microscope.

4 Results

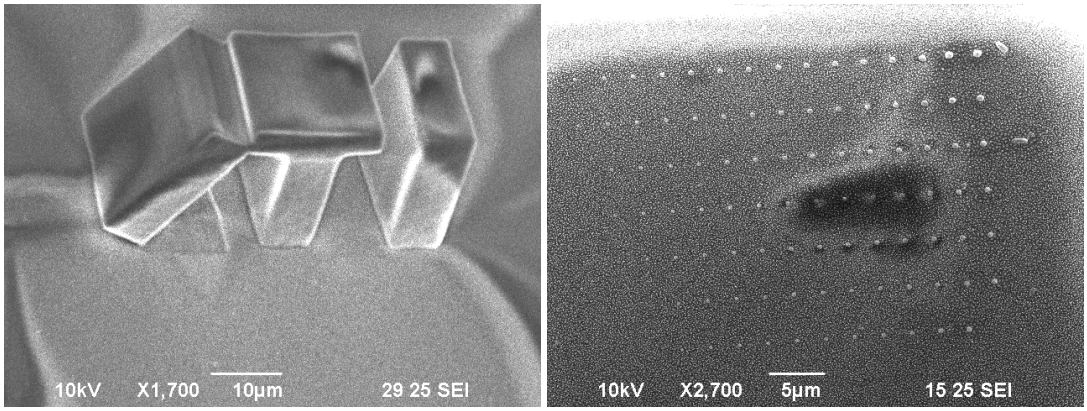

(a) (b)

Figure 4.1: (a) 3D printed LTI logo using the vector scan method (b) Voxel array at a laser power of 1.5W that is used to measure the voxel dimensions for determining the polymerization threshold of the photoresist. Images were generated using an SEM.

The resulting structures that have been written into the resist can be seen in figure 4.1. In figure 4.1 (a), the exposed LTI logo structure can be seen. We speculate that the lower part of the letter L is too thin to support the upper part so that the left part has fallen onto the Letter T probably due to mechanical stress and/or vibrations. Also it could be that the sample has been placed too high, the lower voxels have been placed inside the glass substrate and not inside the resist resulting in the lower part of the structure being cut off.
The voxel array is used for the determination of different growth and exposure parameters. The length of a voxel is determined following an ascending scan method [7]. Inside one row, the exposure time and the laser power is kept constant while the laser focus is shifted in ascending steps of 100 nm. The voxels that lie inside the glass substrate will not be seen, while the ones that lie more than one voxel length away from the substrate will be washed away during development. This way the length of a voxel can be determined in integer multiples of 100 nm by counting the number of visible voxel in a row. The experimental uncertainty using this technique lies in the range of 100 nm. The exposure times in the seven rows is 50 ms, 40 ms, 30 ms, 25 ms, 20 ms, 15 ms and 10 ms, respectively. The diameter of voxels at a certain

exposure time is measured in an SEM as depicted in figure 4.2 and was then averaged.

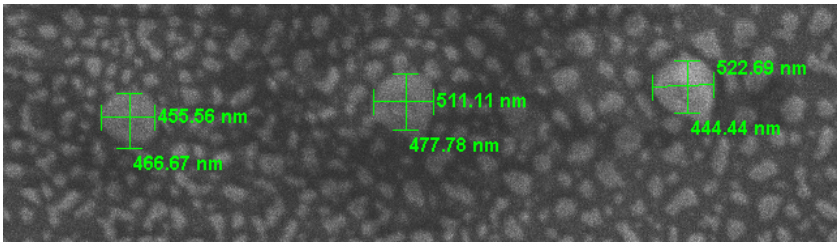

Figure 4.2: SEM image of three voxels with the same exposure time with measurements for the determination of the diameter. P = 0.9W, t_{exp} = 50 ms.

From these measurements we can then derive the relationship of exposure time and power on diameter and length of the voxels. We fitted the data points according to the formulas for length

$$l(N_0,t) = 2z_R[(\frac{\sigma_2 N_0^2 n \tau_L}{C})^{\frac{1}{2}} - 1]^{\frac{1}{2}}$$

and diameter

$$d(N_0,t) = r_0[ln(\frac{\sigma_2 N_0^2 n \tau_L}{C}]^{\frac{1}{2}}$$

as shown before in the theory part. N_0 is proportional to the laser power, while τ_L is proportional to the exposure time.

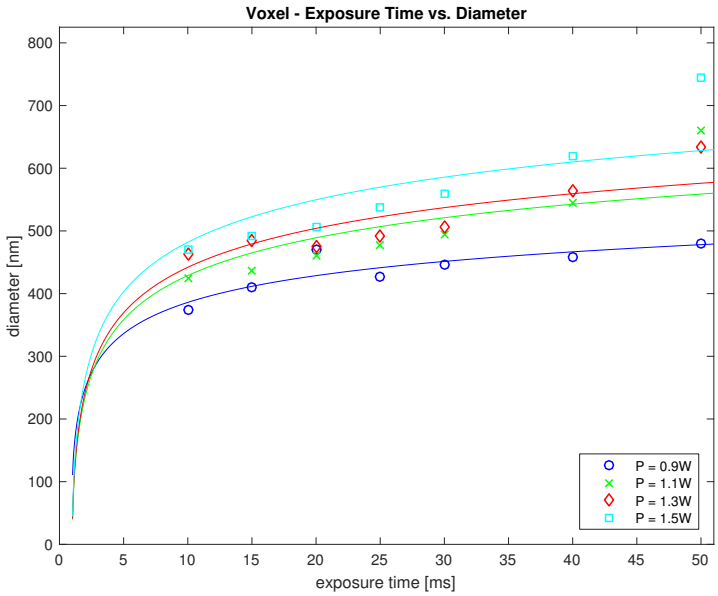

Figure 4.3: Plot of exposure time vs. averaged diameters of voxels for different laser powers. Fitted with $a\sqrt{\ln(b\,x)} + c$.

As seen in Figure 4.3, there is a good agreement between theory and experiment within the uncertainty of the measurement. There were only a few points for high laser power and long

exposure time that has the biggest error compared to the fit. Further examination of the array picture reveals that bigger voxels are more likely to fall over or tilt possibly leading to greater error due to length projection at an angle. We fitted the data points with $a\sqrt{\ln(b\,x)}+c$ with x being the exposure time. There seems to be a saturation behavior where the diameter does not increase much with increasing exposure time. The influence of higher laser power is much higher for the diameter of a voxel than increasing exposure time. But still there is a minimum exposure time needed to develop a certain diameter. Judging from the intersection of the fit with the time axis it is around 1ms. But this should be examined further with more data points as the fit in this region is not very reliable.

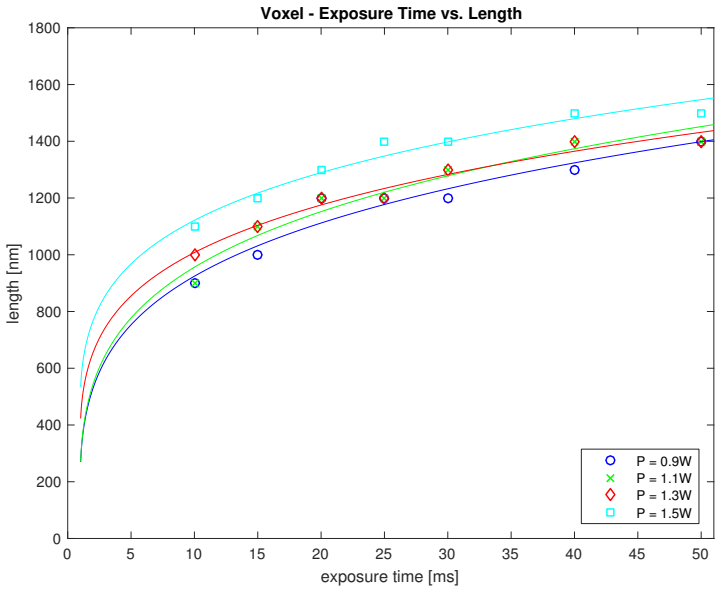

Figure 4.4: Plot of exposure time vs .voxel length for different laser powers. Fitted with $a\sqrt{\sqrt{b\,x}-1}+c$.

Figure 4.4 shows the relationship of exposure time and length. We fitted the plots according to the equation explained before with $a\sqrt{\sqrt{b\,x}-1}+c$. As we have determined the length of the voxels by the ascending scan method there we can only determine the length of the voxels by steps of 100nm and also an error of 100nm. This big uncertainty is probably why we see that the fits for 1.1W and 1.3W almost lie on top of each other. The length depends on the square of laser power which could explain why there is a bigger length difference between the voxels at laser power 1.5W and the one at 1.3W than between the others. However, this could again be due to the big uncertainty of 100nm.
Figure 4.5 shows the relationship of laser power and the diameter with the theoretical fit according to $a\sqrt{\ln(b\,x^2)}+c$ with x the laser power. Since there are only four data points, the fits have big errors. The behavior because of the curves is also counter intuitive. We would expect the curve for exposure time of 50ms to intersect with the power axis at a point much further to the left, that is the voxel should already grow with a lower laser power. This experiment should be repeated to better understand the growth behavior. From these plots it would then be possible to get a minimum threshold laser power needed to grow voxels.

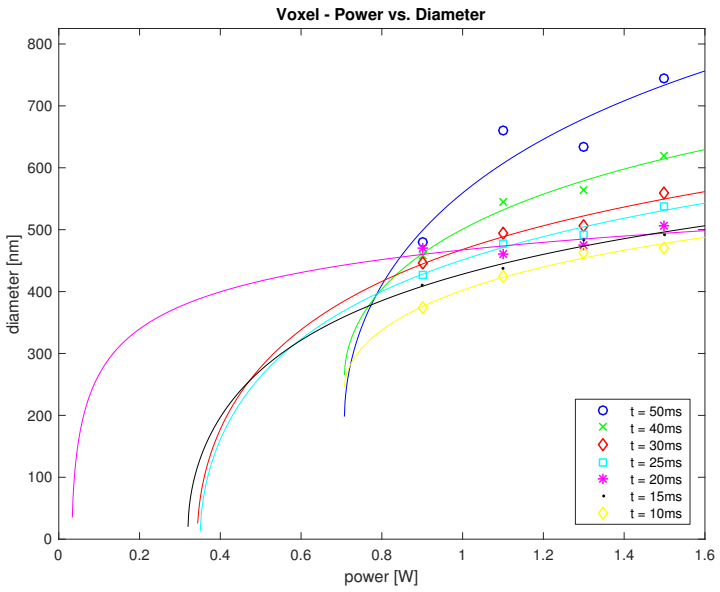

Figure 4.5: Plot of laser power vs. averaged diameters of voxels for different exposure times. Fitted with $a\sqrt{\ln(b\,x^2)}+c$.

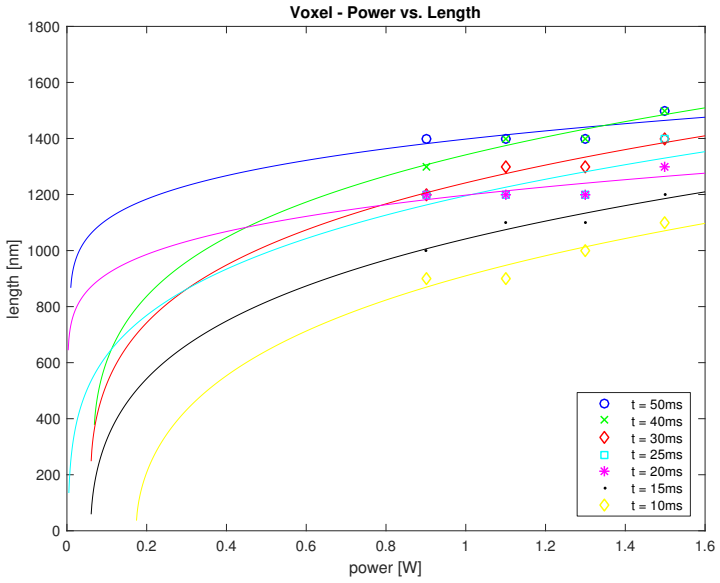

Figure 4.6: Plot of laser power vs. voxel length for different exposure times. Fitted with $a\sqrt{\sqrt{b\,x^2}-1}+c$.

Figure 4.6 depicts the dependence of voxel length to laser power. The data points where fitted according to the length equation with $a\sqrt{\sqrt{b\,x^2}-1}+c$ with x the laser power. Again, there were not many data points available for fitting causing bigger errors. Interestingly, the curves for 40ms and 50ms overlap mostly. This might indicate a saturation behavior with a maximum exposure time of around 40ms that limits the length of the voxels. However, again we are

limited as we have no data at higher exposure times and a resolution of only 100nm with 100nm errors.
It is conceivable than the TPP process takes finite time from excitation of the molecules to complete polymerization. It is also expected to have no polymerization for short exposure times (1 ms according to our fits) because of the time it takes for polymerization to happen and the probability of two photons to be absorbed in a given time period. It would be an interesting investigation to sample shorter exposure times more frequently to better study the polymerization mechanism.

5 Conclusion

In conclusion, we have demonstrated that using the two photon photo-polymerization (TPP) method, 3D structures can be manufactured with voxel sizes even below the diffraction limit. The process can be further improved by investigating different photoresists and introducing concepts from stimulated emission microscopy (STED). In other words, it might be possible to initiate polymerization in some areas using a certain wavelength and inhibit it by using another wavelength to further refine the voxel size. It is possible to prototype 3D metamaterials and optically interesting structures very rapidly and in a cheap way. For example, it is conceivable that plasmonic structures can be fabricated by printing the negatives of the structures with the polymer and then electroplating the exposed parts of the substrate. TPP is also likely to find a wide range of applications in integrated photonics and biomedical sciences.

Bibliography

[1] Scanning electron microscope. https://www.purdue.edu/ehps/rem/rs/sem.htm.

[2] Scanning electron microscope. https://en.wikipedia.org/wiki/Scanning_electron_microscope.

[3] Vik Dhillon. www.vikdhillon.staff.shef.ac.uk/teaching/phy217/telescopes/rayleigh2.gif. Department of Physics and Astronomy University of Sheffield.

[4] Anne Habermehl. *Nanotechnology Laboratory: Direct Laser Writing and Scanning Electron Microscopy*. Light Technology Institute, Karlsruhe Institute of Technology.

[5] Hiroaki Nishiyama and Yoshinori Hirata. Femtosecond laser nonlinear lithography. http://www.intechopen.com/books/lithography/femtosecond-laser-nonlinear-lithography.

[6] J. Serbin, A. Egbert, A Ostendorf, B. N. Chichkov, R. Houbertz, G. Domann, J. Schulz, C. Cronauer, L. Froehlich, and M. Popall. Femtosecond laser-induced two-photon polymerization of inorganic-organic hybrid materials for applications in photonics. *OPTICS LETTERS*, 28(5), March 2003.

[7] Hong-Bo Sun and Satoshi Kawata. Two-photon laser precision micorfabrication and its applications to micro-nano devices and systems. *Journal of Lightwave Technology*, 21(3), March 2003.